



Article

The Effect of the Environment on the Case Hardening Characteristics of AISI 1018 Steel during Cassava Leaf Pack Cyaniding

Renee Erica Gordon ¹, Egwu Eric Kalu ^{2,*}, Adelana Rasak Adetunji ³, Dorr Campbell ⁴ and Peter N. Kalu ⁴

¹ STEM Department, Tallahassee Community College, Tallahassee, FL 32304-2895, USA; renee.gordon@tcc.fl.edu

² Department of Chemical and Biomedical Engineering, FAMU-FSU College of Engineering, Tallahassee, FL 32310-6046, USA

³ Department of Metallurgical and Materials Engineering, Faculty of Technology, Obafemi Awolowo University, Ile-Ife 220282, Nigeria; aderade2004@yahoo.com

⁴ Department of Mechanical Engineering, FAMU-FSU College of Engineering, Tallahassee, FL 32310-6046, USA; dcampbell@eng.famu.fsu.edu (D.C.); kalu@eng.famu.fsu.edu (P.N.K.)

* Correspondence: ekalu@eng.famu.fsu.edu

Abstract: As part of a comprehensive study on eco-friendly processing techniques, the influence of the heat treatment environment on the case hardening of AISI 1018 steel using pulverized cassava leaf was studied. The process was carried out at two different temperatures (850 °C and 950 °C) and under three environmental conditions: Process 1, the control experiment, was carried out in air only; in Process 2, the medium comprised pulverized cassava leaves; and in Process 3 a combination of pulverized cassava leaves plus barium carbonate (BaCO₃) was used as an energizer (CBC mixture). Vickers microhardness testing and scanning electron microscopy were used to evaluate the effect of the processing environment on the case hardening of the steel. As expected, regardless of the processing temperature, Process 1 resulted in little or no hardening of the steel surface. However, notable case hardening occurred when the steel specimens were subjected to either Process 2 or Process 3. Furthermore, the inclusion of barium carbonate in Process 3 significantly enhanced the case hardening effectiveness of the cassava leaf in terms of the rate of and maximum hardness achieved. A maximum enhancement was observed at 950 °C. After 1 h, the increase in hardness was 160% and 280% for Process 2 and Process 3, respectively. Upon increasing the processing time to 5 h, the increase in hardness due to Process 2 was raised to 254%, while that of Process 3 remained at approximately 280%. The diffusivity of AISI 1018 was calculated using the microhardness data. The diffusivity was highest in Process 2 samples with values of 1.568×10^{-9} m²/s at 850 °C and 1.893×10^{-9} m²/s at 950 °C. Effective case hardening of AISI 1018 steel was carried out using the medium of cassava leaf, without the addition of barium carbonate (BaCO₃) as an energizer.

Keywords: case hardening; surface treatment; diffusion; cassava; steel microstructure; microhardness



Citation: Gordon, R.E.; Kalu, E.E.; Adetunji, A.R.; Campbell, D.; Kalu, P.N. The Effect of the Environment on the Case Hardening Characteristics of AISI 1018 Steel during Cassava Leaf Pack Cyaniding. *Alloys* **2024**, *3*, 1–14. <https://doi.org/10.3390/alloys3010001>

Academic Editor: Seok Su Sohn

Received: 30 November 2023

Revised: 23 December 2023

Accepted: 28 December 2023

Published: 31 December 2023



Copyright: © 2023 by the authors. Licensee MDPI, Basel, Switzerland. This article is an open access article distributed under the terms and conditions of the Creative Commons Attribution (CC BY) license (<https://creativecommons.org/licenses/by/4.0/>).

1. Introduction

Many developing countries have an acute shortage of spare parts and components for maintenance work, especially in the automobile industry. With high local exchange rates, the importation of such spare parts in these countries has become virtually untenable [1].

Gear teeth, camshafts, and some other automobile components need good surface hardness to resist wear, in combination with considerable interior toughness to withstand impact [2–4]. These components are generally manufactured by surface or case hardening of mild steel. Case hardening is an immensely broad area of study, spanning many modes of processing. The case hardening of steel is a vastly utilized surface treatment process. It relies on the diffusion of carbon and/or nitrogen into the surface of steel specimens,

followed by a suitable heat treatment. The process is conducted by putting the steel in a carbon-rich and/or nitrogen-rich atmosphere at elevated temperatures. This results in the interstitial diffusion of the carbon and/or nitrogen into the steel surface so that the steel surface may be hardened, thereby increasing the material's surface hardness and wear resistance [5]. A major drawback of conventional case hardening is the potentially hazardous nature of the process, particularly with the use of sodium cyanide salts [6].

To address some of the disadvantages of conventional case hardening, alternative methods utilizing organic biomass have been considered. In some cases, coffee grinds, sea shells, and cow bones have been shown to successfully case-harden mild steel [7–9]. Oliver et al. [7] showed that there was a consistent change in the hardness of mild steel case hardened with Blue Mountain coffee grinds, where the optimal processing time for achieving maximum case hardness changed with temperature. The results demonstrate that utilizing biomass does not change the multi-variable nature of the case hardening process. Ihom [8] verified that incorporating 40 wt.% cow bone into the case hardening of mild steel resulted in a hardness value of 950 HV at 0.2 mm (case region) and 358 HV at 4 mm (core region). Akanji et al. [9] achieved an optimal carburizing (case hardening) effect (310 HV) of mild steel using 90% charcoal and 10% seashell at a 212 µm particle size with an 8 hr processing time before quenching with water. The pack cyaniding of mild steel using the cyanide product from the cassava leaf has been previously investigated [10]. Ibrinke et al. [10] examined the use of cassava leaf in cyaniding (case hardening) of mild steel at a single temperature (860 °C) and developed a mathematical model of the process. Unlike the present work, they did not consider varying temperatures or the effect of an energizer on the cassava cyaniding process. These greener processes, as additional options for enhancing the mechanical properties of materials, has been demonstrated by previous studies through the quantification of surface microhardness and carbon concentration profiles [11–13].

The objective of this work is to assess the major parameters which influence the pack cyaniding effectiveness of cassava leaf with respect to its holding time, processing temperature, and medium/environment. A common practice in pack cyaniding is to add an energizer or catalyst to the pulverized cassava leaf to accelerate the case hardening process—typically barium carbonate (BaCO_3). It provides additional nascent carbon, thereby increasing the diffusion potential for case hardening [14]. This study explored the use of cassava leaf alone (without energizer) as well as in combination with an energizer, to verify its effectiveness in case hardening. In addition, the effect of varying temperatures was explored.

Decomposition of Cassava

Cassava (*Manihot esculenta*) is an important food and source of starch to at least 500 million people in tropical and subtropical regions [15]. Several studies have been conducted using cassava waste (leaves and peels) to improve the surface hardness of steels [16]. This is due to the activated carbon available in cassava biomass [17–20]. Upon the tissue disruption of cassava leaf, a release of cyanogenic glucosides (CNGs) is activated [21]. This acts as a defense mechanism for the plant against herbivore attacks [22]. Linamarin, the dominant type of CNG, is brought into contact with the enzyme linamarase when cassava leaf is subjected to chewing or grinding, and produces the compound acetone cyanohydrin [23]. Acetone cyanohydrin is then enzymatically broken down by hydroxynitrile lyase (HNL) [24]. Finally, the HNL degrades to produce acetone and hydrogen cyanide, along with additional chemical by-products, as outlined in Figure 1. The hydrogen cyanide (HCN) produced becomes the active ingredient for the pack cyaniding and case hardening of steel.

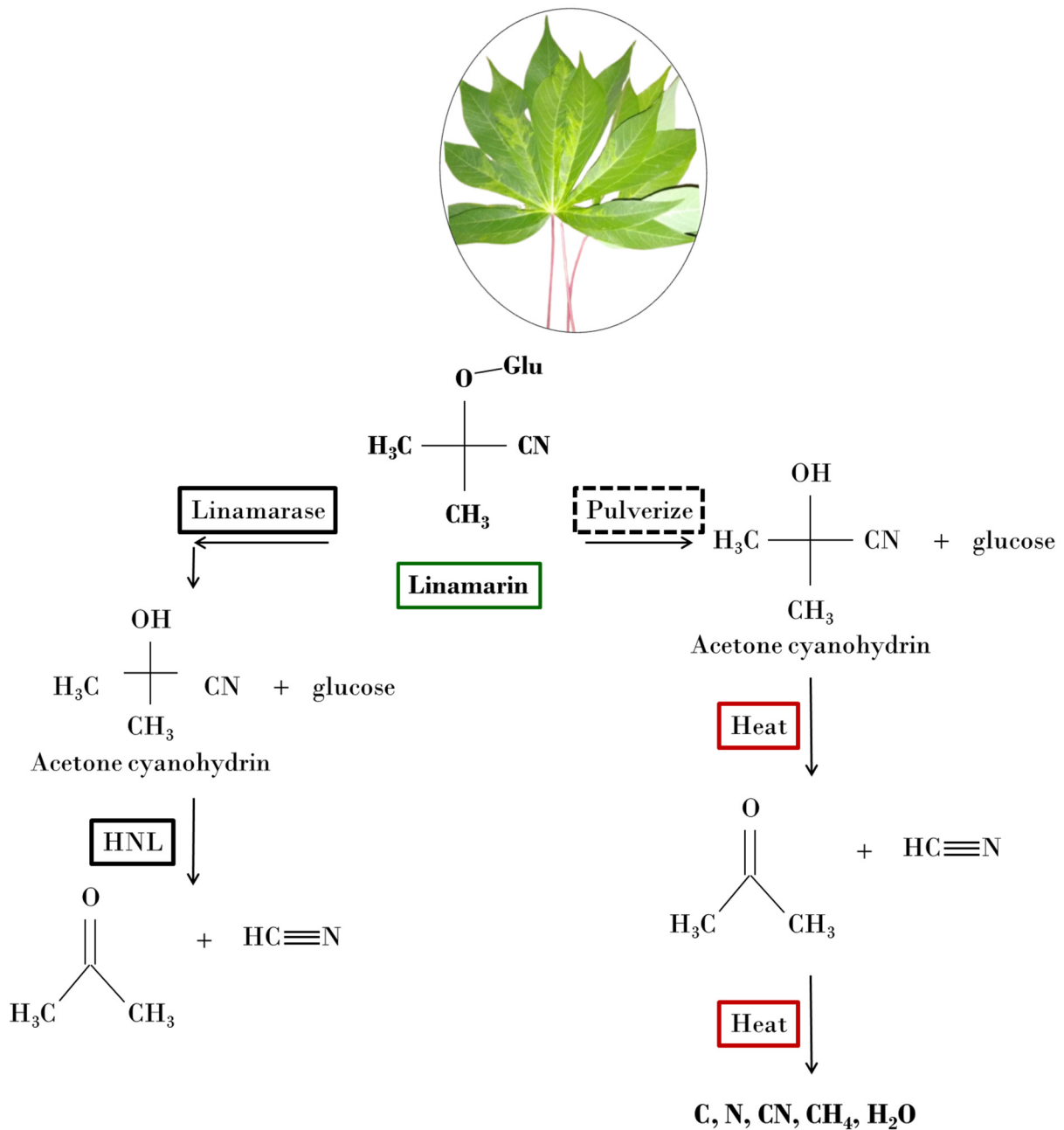


Figure 1. Catabolism of linamarin in cassava (*Manihot esculenta*) to produce hydrogen cyanide (**left**). Hydroxynitrile lyase (HNL) converts acetone cyanohydrin to hydrogen cyanide. This is compared with the thermal decomposition of the linamarin in cassava due to pulverization, with a subsequent high temperature to produce experimental diffusing species (**right**).

As a substitution for the enzymatic decomposition of cassava, an elevated temperature can act as a decomposing mechanism in the production of acetone and hydrogen cyanide from cassava. This is similar to the tissue disruption that occurs during herbivore attacks. The biological breakdown is replaced by a thermochemical breakdown. In the case of the cassava leaf case hardening process, heat acts as a substitute to the linamarase enzyme. High temperatures (850–950 °C) further reduce acetone and hydrogen cyanide into carbon, nitrogen, methane, and water vapor (Figure 1). These thermally produced constituents will be explored for the pack cyaniding of AISI 1018 steel.

2. Experimental Section

Low-carbon AISI 1018 was selected for this study and its chemical composition is given in Table 1. The steel was machined into cube-shaped pieces of approximately 12 mm length on each side.

Table 1. Chemical composition of low carbon AISI 1018 steel (wt.%).

C	Mn	Si	P	S
0.15–0.20	0.60–0.90	0.15–0.30	0–0.04	0–0.05

Fresh cassava leaves were cut, dehydrated, and then pulverized using a mortar and pestle. Pulverization of the cassava leaf produced an average powder particle size of 0.6 mm. In order to determine if the pulverized cassava leaf had any effect on the properties of the steel, three processing conditions were used, as shown in Table 2. Process 1, which was used as the control, involved the heat treatment of the steel in air (with no cassava leaf present). This baseline experiment provided a means to assess the influence of the processing media/environment. Process 2 involved the heat treatment of the steel in contact with pulverized cassava leaf. Process 3 was carried out in the presence of pulverized cassava leaf with BaCO₃ as an energizer (CBC mixture). The ratio of pulverized cassava leaf to BaCO₃ energizer was 4:1 by weight.

Table 2. Summary of experimental processing parameters. Holding time, processing temperature, medium/environment, and process identification names are specified.

Process Identification	Medium/Environment	Details
Unprocessed	N/A	As-received AISI 1018 steel.
Process 1	Air	Heat treatment of AISI 1018 steel in air (with no cassava leaf present).
Process 2	Pulverized Cassava Leaf	Heat treatment of AISI 1018 steel in pulverized cassava leaf.
Process 3	Pulverized Cassava Leaf + Barium Carbonate (BaCO ₃) * also called the “CBC Mixture”	Heat treatment of AISI 1018 steel in pulverized cassava leaf with BaCO ₃ as energizer (CBC mixture). The ratio of pulverized cassava leaf to energizer was 4:1 by weight.
	Temperature (°C)	Holding Time
	850	1 h
		5 h
	950	1 h
		5 h

For processing, samples were packed into a mild steel metal boat. The metal boat lid was sealed using fire clay and placed into a Gallenkomp Muffle Furnace (SXL-1008) (Cambridge, United Kingdom) at temperatures of 850 °C and 950 °C, for time periods 1 h and 5 h (Table 2).

The Fe-C phase diagram provides important temperature–composition information. When the ferrite–pearlite structure transforms to the austenite phase, this is designated as the A₃ transformation temperature. For AISI 1018 steel, the A₃ transformation temperature occurs at approximately 870 °C. It is important to recognize that above 870 °C, the AISI 1018 steel completely transforms to its austenite phase. Therefore, all samples processed at 950 °C had an austenite microstructure during heat treatment. Once removed from the furnace, the steel samples were immediately quenched in room temperature water.

The pack cyanided samples were prepared for microhardness testing and metallographic examination by cold-mounting and surface grinding to the fineness of P-4000 silicon

carbide paper. Polishing was carried out using a Buehler Vibromet 2 vibratory polisher with 0.25 μm OP-S solution for 4 h. Samples were immersed in a 3% nital etchant, and then sprayed with deionized water and air dried. A Tukon 2100 Vickers microhardness tester was used with a 300 g applied load and a dwell time of 10 s to obtain near-surface microhardness profile measurements. This was analyzed with respect to the distance/depth from the outer surface. Sample microstructure was examined utilizing the Zeiss 1540 EsB dual beam field emission Scanning Electron Microscope. Energy Dispersive X-ray Spectroscopy (EDS) was performed using the same system. Thermodynamic calculation software was used as a speculative tool to identify the phases present in AISI 1018. Computations were performed using the TCFE8 database, which included steel and iron alloys.

3. Results and Discussion

3.1. Microhardness Profiles

In order to establish a baseline control for the study, low-carbon AISI 1018 steel was heat treated in air at 850 $^{\circ}\text{C}$ and 950 $^{\circ}\text{C}$ and quenched in room temperature water (Process 1). When using Process 1 for any combination of the various experimental conditions (Table 2), there was no significant dissimilarity in the cross-section microhardness of the steel. For Process 1, the average microhardness values of AISI 1018 steel were 243.6 ± 3.3 HV and 272.1 ± 8.1 HV for 850 $^{\circ}\text{C}$ and 950 $^{\circ}\text{C}$, respectively. A comparison of the microhardness of all samples subjected to the Process 1 heat treatment and the as-received material is shown in Figure 2. In addition to being uniform across the thickness, the microhardness profiles of the Process 1 materials were very similar to that of the as-received material. This clearly shows that the steel used in this study does not exhibit any form of hardenability without assistance from a medium/environment.

The influence of the processing medium/environment on the microhardness profile for heat treatments carried out at 850 $^{\circ}\text{C}$ can be seen in Figure 2a,b. In contrast to Process 1, the microhardness profiles of both Process 2 and Process 3 are characterized by three regions: high microhardness surface regions (case); a transition region where the microhardness decreased gradually; and then finally an unaffected, softer, interior region (core). Employing Process 2 for the holding time of 1 h produced a microhardness value of approximately 534.2 ± 28.8 HV and 245.1 ± 45.4 HV in the case and core regions, respectively. However, when Process 3 was utilized with the same 1 h time condition, the case microhardness increased to 852 ± 63.2 HV, while the core remained low at 256.9 ± 50.5 HV. The depth of the case regions for either condition was less than about 600 μm . Increasing the heat treatment time to 5 h increased the case microhardness marginally, but significantly increased the depth of the case region to more than 700 μm for both Process 2 and Process 3. It is evident that Process 3, with the addition of the BaCO_3 energizer to the pulverized cassava leaf (CBC mixture) resulted in a higher microhardness in the case region.

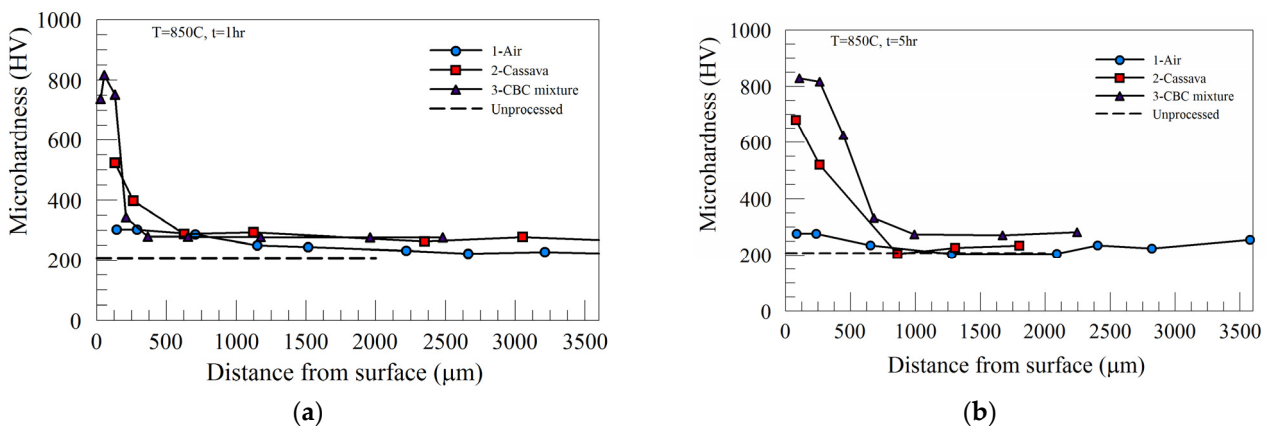


Figure 2. Cont.

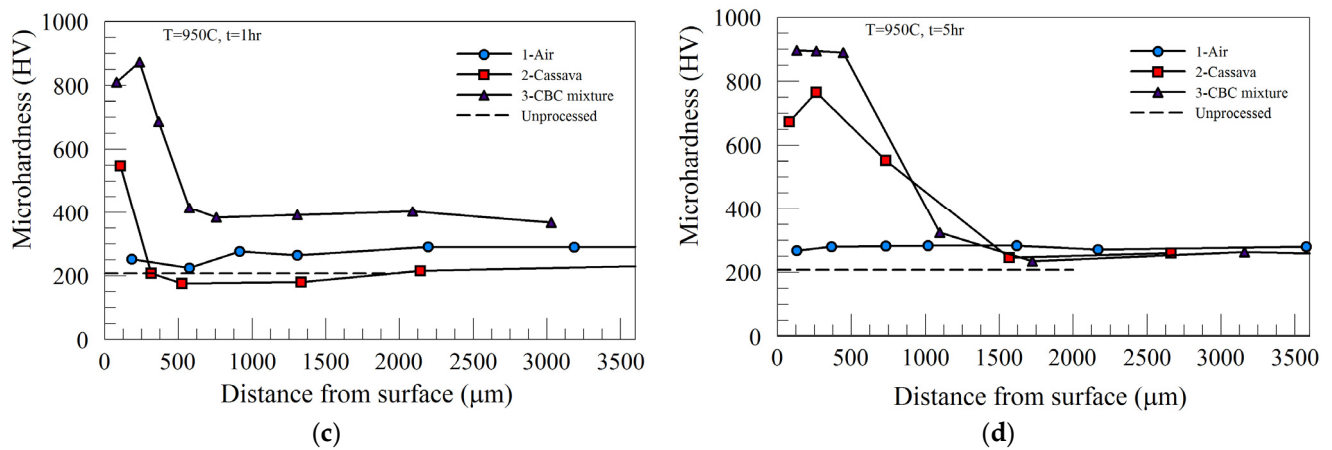


Figure 2. Microhardness profiles of AISI 1018 as received (unprocessed), in air (Process 1—air), pulverized cassava leaf (Process 2—cassava), and pulverized cassava leaf + BaCO₃ (Process 3—CBC mixture) at (a) 850 °C for 1 h processing time; (b) 850 °C for 5 h processing time; (c) 950 °C for 1 h processing time; and (d) 950 °C for 5 h processing time.

Increasing the processing temperature to 950 °C, the temperature at which complete austenitic steel transformation occurs, produced a higher peak microhardness in the case region for both Process 2 and Process 3. However, the microhardness profiles across the specimen thickness and the values of the core microhardness were similar to those of 850 °C. A summary of the peak microhardness and the case depth as a function of processing time for Process 2 and Process 3 are provided in Figure 3a,b, respectively. While the peak microhardness of Process 2 increased with the processing time, there was little or no effect of the heat treatment time on the peak microhardness of the materials heat-treated using Process 3 (see Figure 3a). Furthermore, Process 3 (CBC mixture) carried out at 950 °C produced the highest microhardness value (~900 HV), which was about the same regardless of either holding time used in this study.

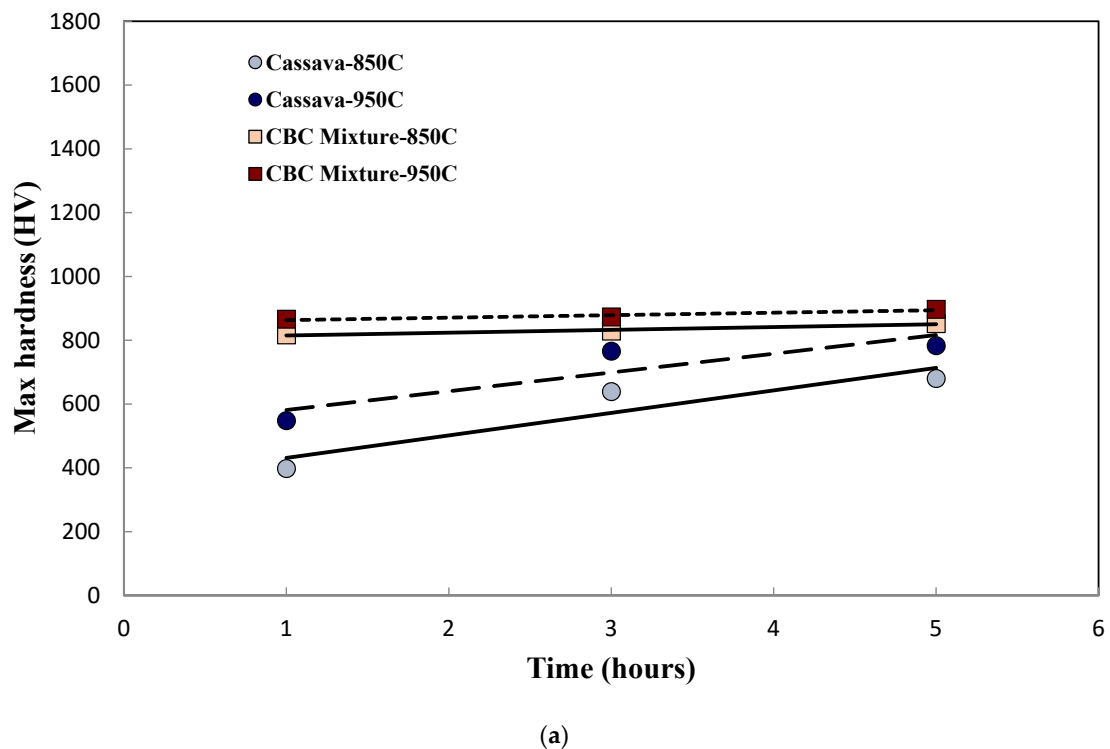


Figure 3. Cont.

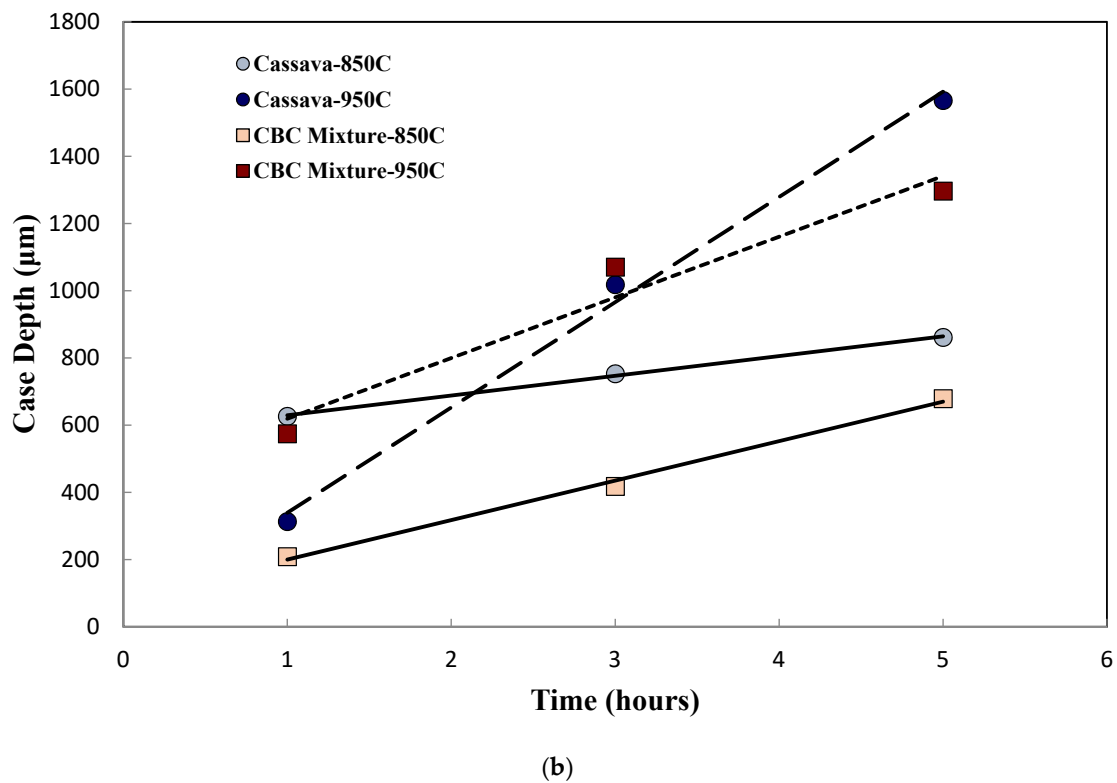


Figure 3. Graphs for AISI 1018 processed in pulverized cassava leaf (cassava) and pulverized cassava leaf + BaCO₃ (CBC mixture) displaying (a) maximum microhardness with respect to time and (b) case depth with respect to time.

The experimental parameters of holding time, temperature, and medium/environment were assessed to understand the level of their effect on the steel sample's hardness. For Process 2, the difference in peak microhardness (Δh_{\max}) between 950 °C and 850 °C was ~103 HV, while that for Process 3 was ~45 HV. From Figure 3b, it can be seen that the case depths resulting from Process 2 and Process 3 increased with heat treatment time. While the magnitude and rate of increase in the case depth were more pronounced for processing carried out at 950 °C, those of 850 °C were gradual. This suggests that the case depth was more dependent on the heat treatment temperature than the processing medium/environment.

3.2. Microstructure

As noted, the A₃ transformation temperature occurs when the ferrite–pearlite structure transforms to its austenite phase, which is ~ 870 °C for AISI 1018 steel. Therefore, the choice of 850 °C and 950 °C provides an assessment of the effect of processing below and above the A₃ transformation temperature, respectively. The microstructure of AISI 1018 is a combination of ferrite and austenite at 850 °C, while at 950 °C the steel specimen is completely transformed into austenite (γ -iron) [25]. It is important to recognize that the maximum solubility of carbon in steel at 850 °C and 950 °C is approximately 0.25 wt.% and 1.4 wt.%, respectively. While a substantial amount of interstitial solute atoms (particularly carbon) will diffuse from the atmosphere into the steel matrix when processed at 950 °C, the inverse is true at 850 °C.

Scanning electron micrographs of as-received and processed AISI 1018 are presented in Figures 4 and 5. The as-received microstructure in Figure 4a is characterized by a ferrite and pearlite structure. Upon processing in an air-only medium (Process 1), the microstructure characteristics exhibited no significant change, as shown in Figure 4b. The observation made for specimens processed in pulverized cassava leaf (Process 2—cassava) was different than the result seen in Figure 4b. Unlike Figure 4b, the near-surface

(case region) microstructure of samples that underwent Process 2—cassava consist of fine platelets, as shown in Figure 5a. The microstructure of the core region, shown in Figure 5b, does not exhibit the characteristics of the case region. A comparison of the microstructure in Figure 5a with the microstructure of SA508 Grade 3 steel austenitized at 1150 °C and cooled above 10 °C, as shown in Figure 4a,b of reference [15], shows a lot of similarities in its microstructure. This suggests that Process 2—the cassava treatment—in this work resulted in the formation of martensite near the surface (case region), as shown in Figure 5a, where the fine platelets are arranged in martensitic platelets [26]. The microstructure of the core region of the same sample is characterized by ferrite and pearlite (Figure 5b). Samples processed in pulverized cassava leaf + BaCO₃ (Process 3) resulted in a similar microstructure to that of pulverized cassava leaf (Process 2).

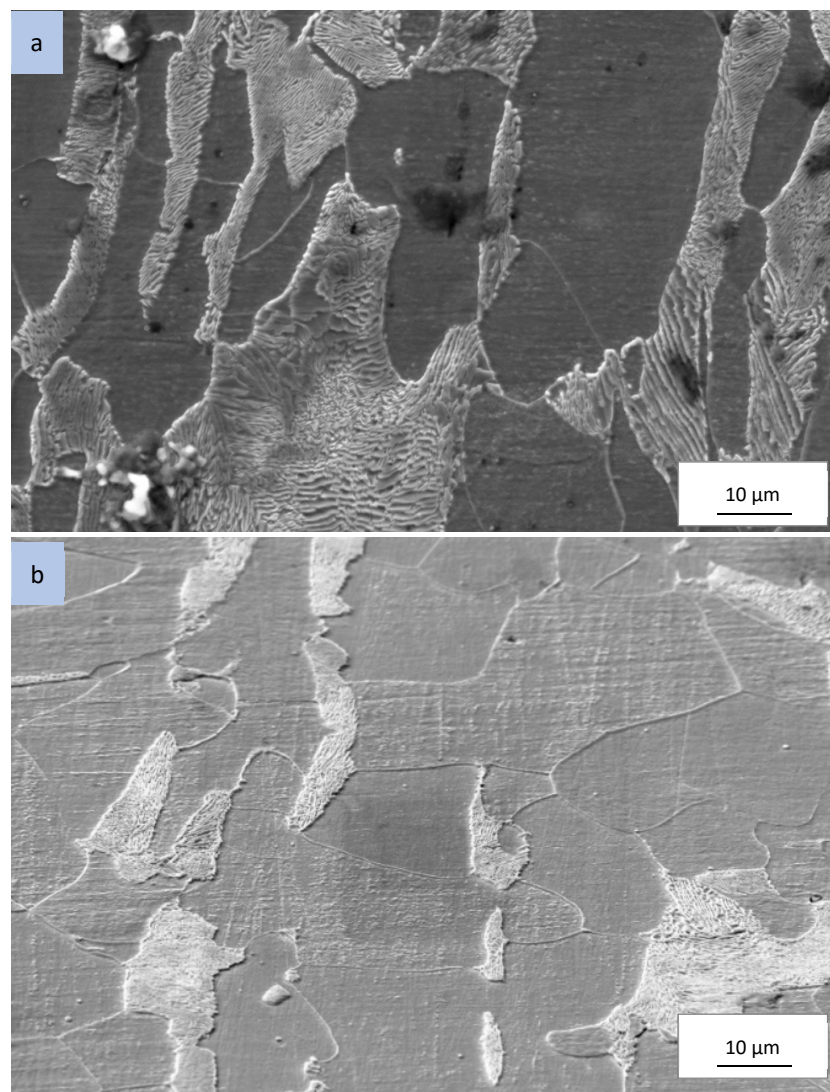


Figure 4. Scanning electron micrograph of AISI 1018 in the (a) as-received condition. The micrograph is characterized by a pearlite and ferrite structure. A similar pearlite and ferrite microstructure is shown in (b) after processing in air (Process 1) at 950 °C for 5 h.

The microstructure results correlate well with the microhardness data for all processes. It is evident that the ferrite and pearlite microstructure was responsible for the low microhardness values present in the core region for all processing conditions. In contrast, the martensite microstructure within the case region produced a high microhardness. As martensite is present in the Process 2 and Process 3 samples, a martensitic transformation is the hardening mechanism.

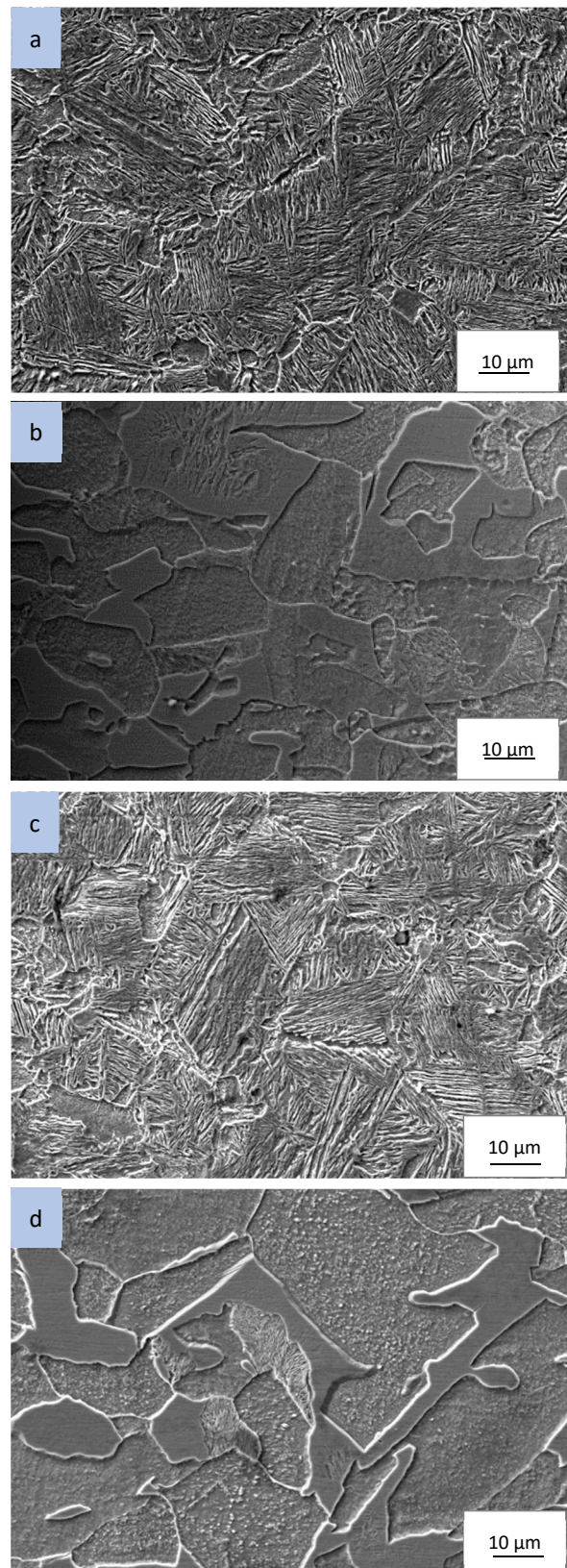


Figure 5. Scanning electron micrograph of AISI 1018 processed at 950 °C for 5 h in pulverized cassava leaf (Process 2) at (a) case region at $x = 250 \mu\text{m}$ and (b) core region at $x = 2000 \mu\text{m}$, where x denotes a distance from the surface. CBC mixture (Process 3) micrographs were similar to those of pulverized cassava leaf (Process 2). The case region (c) formed martensite and the (d) core region was characterized by a pearlite and ferrite microstructure.

It has been discussed that the addition of BaCO₃ to the CBC mixture as a source of nascent carbon resulted in an increase in the maximum hardening. However, the processing temperature had a greater effect on the maximum hardness. This can possibly be attributed to the high temperature required for the breakdown of barium carbonate. At approximately 1260 K (~986 °C) the onset of the decomposition reaction of barium carbonate begins: BaCO₃ (solid) = BaO (solid) + CO₂ (gas) [27]. The CO₂ gas and its derivatives increase the carbon potential of the atmosphere, making it greater than the carbon potential at the surface of the specimen. Experimental temperatures did not exceed 950 °C, therefore the complete decomposition of barium carbonate was not achieved.

It has been established from other studies that microhardness can be used to assess the amount of solute present in the steel matrix. In the absence of precipitation, the microhardness gradient can only be caused by the concentration gradient within the microstructure. Therefore, one can use the microhardness value as a means of assessing the carbon concentration of the material.

3.3. Diffusion of Pulverized Cassava Leaf Media in Steel

The atmosphere at the steel sample's surface during Process 2 and Process 3 is rich in carbon and thus presents a concentration gradient for carbon at the surface versus the interior. The carbon concentration gradient can be approximated using Fick's second law, whose governing equations for the one-dimensional case are

$$\frac{\partial C}{\partial t} = D \frac{\partial^2 C}{\partial x^2} \quad (1)$$

$$C(x, t) = \frac{1}{2\sqrt{\pi Dt}} \exp\left(\frac{-x^2}{4Dt}\right) \quad (2)$$

where C is the concentration, D is the diffusion coefficient dependent on the temperature but independent of species composition, t is time, and x is the distance from the material's surface. It is assumed that the concentration of carbon in the case hardened steel is proportional to its relative microhardness, such that

$$C(x, t) = \frac{h - h_0}{h_s - h_0} \quad (3)$$

where h_s is the maximum microhardness near the contact surface, h_0 is the lowest microhardness of the untreated steel (230 HV), h is the microhardness at any distance x from the contact surface, and H is defined as the relative microhardness. This assumption is based on previous research, which demonstrates that through the examination of carbon diffusion in steel, the carbon content can be replaced by microhardness [28,29].

The correlation between concentration and microhardness can yield a simple analytical model to express the effect properties of steel encountered during cassava leaf case hardening. On linearizing Equation (3) with respect to x^2 , a plot of $\ln(H)$ versus x^2 for each processing temperature of the experiment is obtained. Diffusion coefficients were calculated from the slopes of these lines and are presented in Table 3. The effect of temperature on diffusivity is apparent. Increasing the temperature is the most effective parameter in improving surface hardness and diffusivity growth. In the work of Grube and Gay, plasma carburization was conducted on AISI 1018 at 1050 °C—yielding a diffusivity of $1.6 \times 10^{-10} \text{ m}^2/\text{s}$ [30]. This is within a 10% difference to the obtained diffusivity rates of the present work. Using the diffusion coefficients in Table 3, carbon concentration with respect to distance from sample surface was estimated for the samples of AISI 1018 processed under different environmental conditions at 950 C for 5 h as shown in Figure 6. Results in Figure 6 indicate higher carbon penetration in the CBC sample than the cassava only treated sample.

Table 3. The diffusion coefficients of AISI 1018 processed in pulverized cassava leaf and the CBC mixture.

Medium/Environment	Temperature (°C)	D (10 ⁻⁹ m ² /s)
Pulverized Cassava Leaf (Process 2)	850	1.568
	950	1.893
Cassava + BaCO ₃ (Process 3)	850	0.177
	950	0.844

Carbon Concentration - AISI 1018

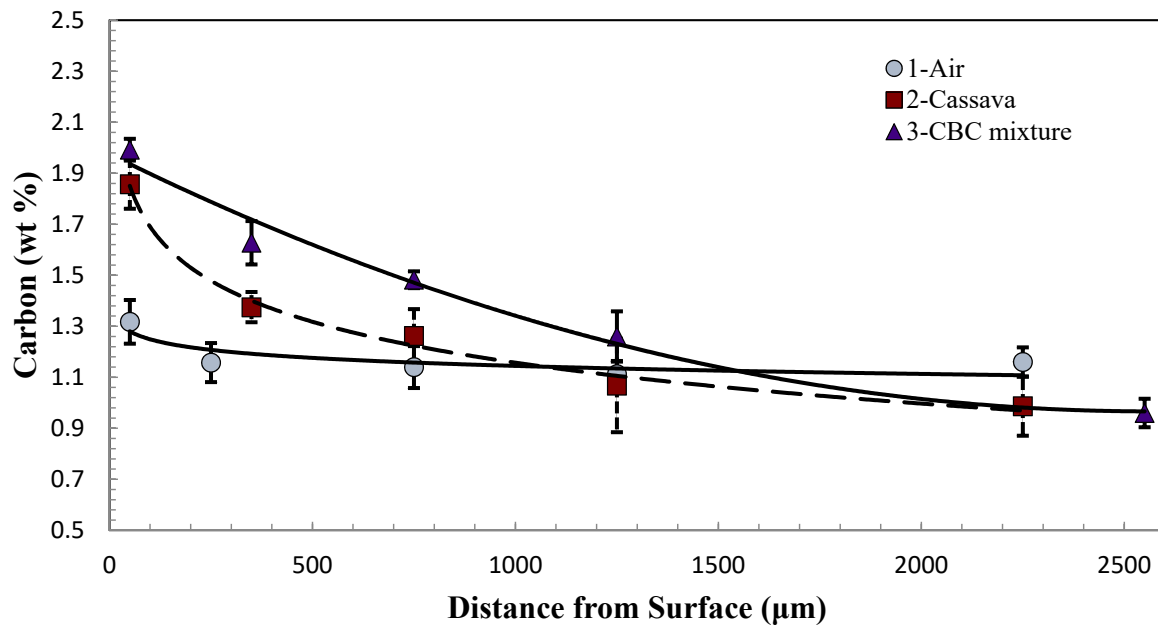


Figure 6. Carbon concentration with respect to the distance from surface of AISI 1018 processed in various media, at a treatment temperature of 950 °C for 5 h.

From Figure 3, pulverized cassava leaf as the processing medium (Process 2) produced an increase in surface hardness (Figure 3a) with a generally large case depth (Figure 3b). Treatment with the CBC mixture (Process 3) produced a markedly higher microhardness than that of Process 2 (Figure 3a). The CBC mixture (Process 3) also yielded a slightly thinner case depth, particularly at 850 °C (Figure 3b). Table 3 reveals that the CBC mixture (Process 3) rendered a significantly reduced diffusion coefficient in comparison to pulverized cassava leaf (Process 2). The addition of barium carbonate increased the carbon available for diffusion in Process 3; however, it reduced the rate of diffusion by up to a factor of ten.

The development of the case layer can be described using Fick's second law with a fixed boundary condition, where the distance of penetration is proportional to the square root of time, expressed by

$$x_{depth} = a\sqrt{Dt} = K\sqrt{t} \quad (4)$$

where x_{depth} is the case layer's thickness, a is a constant, t is the treatment time, D is the diffusion coefficient in the case layer, and K is related to D . Figure 7 displays the case depth (x_{depth}) as a function of the square root of time ($t^{1/2}$) for AISI 1018 processed in pulverized cassava leaf (Process 2) and the CBC mixture (Process 3) at 850 °C and 950 °C. As the

treatment time increases, the case depth is increased. The growth kinetics of the case layer can be described by

$$x_{depth} = 188.77t^{1/2} + 434.19, \text{ for Cassava at } 850 \text{ }^{\circ}\text{C} \quad (5)$$

$$x_{depth} = 1009.87t^{1/2} - 706.77, \text{ for Cassava at } 950 \text{ }^{\circ}\text{C} \quad (6)$$

$$x_{depth} = 373.24t^{1/2} - 183.11, \text{ for CBC at } 850 \text{ }^{\circ}\text{C} \quad (7)$$

$$x_{depth} = 590.83t^{1/2} + 1.73, \text{ for CBC at } 950 \text{ }^{\circ}\text{C} \quad (8)$$

where x_{depth} is in μm and t is in hours. From Equations (5)–(8) it is apparent that the K value increases with temperature, which is fitting as the diffusion coefficient also increases.

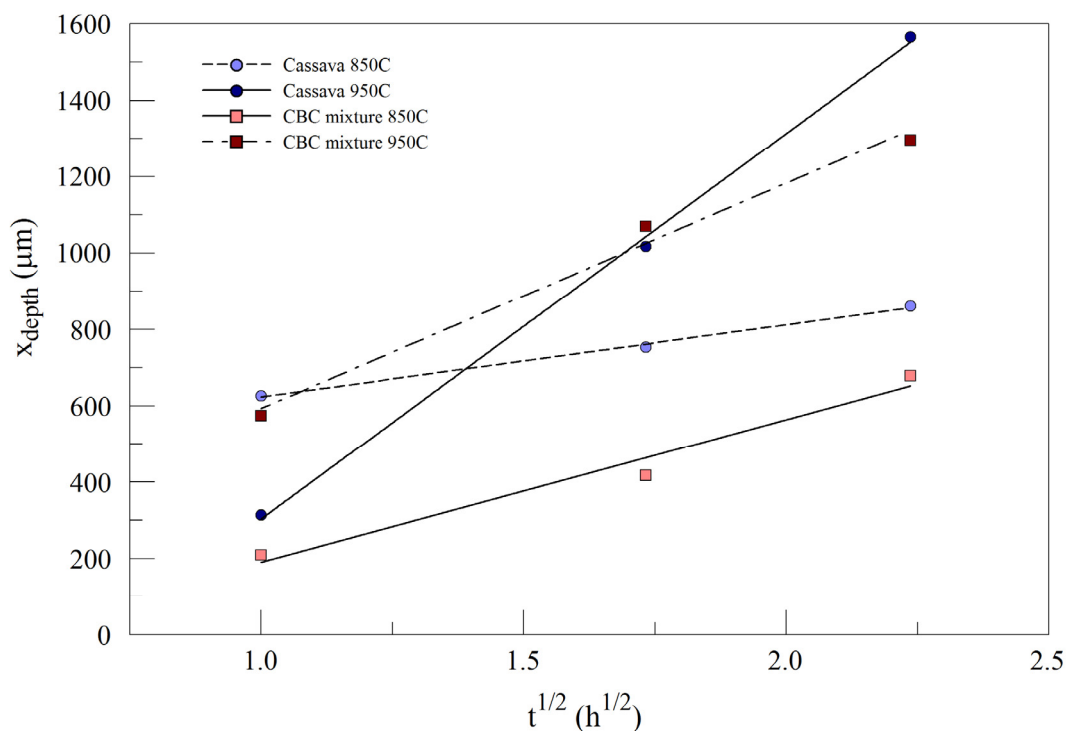


Figure 7. Case depth (x_{depth}) as a function of the square root of time ($t^{1/2}$) for AISI 1018 processed in pulverized cassava leaf and CBC mixture, at 850 °C and 950 °C.

4. Conclusions

The case hardening of AISI 1018 steel using pulverized cassava leaf was studied. The process was carried out at processing temperatures 850 °C and 950 °C and under three environmental conditions: Process 1, as the control experiment, in air only; Process 2, in pulverized cassava leaf; and Process 3, in a combination of pulverized cassava leaf with barium carbonate (BaCO_3) as an energizer (CBC mixture).

1. There was little or no change in the microhardness profile of AISI 1018 steel that was heat-treated in air (Process 1). However, a significant difference in hardness between the surface region and the interior was observed when the steel was processed in either pulverized cassava leaf (Process 2) or the mixture of pulverized cassava leaf and BaCO_3 (Process 3). This confirms that the environment/medium containing cassava leaf (without energizer) resulted in the effective case hardening of AISI 1018 steel.
2. At the completion of Process 2 and Process 3, in AISI 1018 steel, the case depth was found to be lower when the holding temperature was below the A_3 transformation temperature.

3. The addition of the barium carbonate (BaCO_3) energizer (Process 3) produced the highest peak microhardness values (h_{max}), and resulted in the most rapid attainment of maximum case hardness, compared to Process 2. The average difference in peak microhardness (Δh_{max}) between Process 3 and Process 2 was above 100 HV for all samples.
4. Process 2 resulted in a higher rate of diffusion compared to Process 3. Process 2 produced the deepest case depth of 1566 μm at 950 $^\circ\text{C}$ for 5 h.
5. The microstructure of AISI 1018 after Process 2 and Process 3 was characterized by martensite platelets in the case region, while the core region retained its combined ferrite and pearlite microstructure.

Author Contributions: Conceptualization, P.N.K., A.R.A., E.E.K. and R.E.G.; methodology, P.N.K., A.R.A. and R.E.G.; validation, R.E.G., P.N.K. and E.E.K.; formal analysis, P.N.K., E.E.K., A.R.A., D.C. and R.E.G.; investigation, R.E.G.; resources, P.N.K. and A.R.A.; data curation, R.E.G.; writing—original draft preparation, R.E.G.; writing—review and editing, P.N.K., E.E.K. and D.C.; visualization, R.E.G.; supervision, P.N.K., A.R.A. and E.E.K.; project administration, P.N.K. All authors have read and agreed to the published version of the manuscript.

Funding: This research received no external funding.

Data Availability Statement: The original contributions presented in the study are included in the article, further inquiries can be directed to the corresponding author.

Acknowledgments: Renee Erica Gordon gratefully acknowledges financial support for this research from the Fulbright U.S. Student Program, which is sponsored by the U.S. Department of State. The National High Magnetic Field Laboratory (NHMFL) in Tallahassee, Florida, USA, provided scanning electron microscopy (SEM) facilities. For the work conducted in Nigeria, the experimental facility was provided by the Prototype Engineering Development Institute (PEDI), a financially supported institute of the National Agency for Science and Engineering Infrastructure (NASENI). This article's contents are solely the responsibility of the authors and do not necessarily represent the official views of the Fulbright Program or the Government of the United States.

Conflicts of Interest: The authors declare no conflicts of interest. The funders had no role in the design of the study; in the collection, analyses, or interpretation of data; in the writing of the manuscript; or in the decision to publish the results.

References

1. Adetunji, A.R. Metallographic Studies of Pack Cyanided Mild Steel Using Cassava Leaves. *Mater. Manuf. Process.* **2008**, *23*, 385–390. [[CrossRef](#)]
2. Schmitt, M.; Gerstl, F.; Boesele, M.; Horn, M.; Schlick, G.; Schilp, J.; Reinhart, G. Influence of Part Geometry and Feature Size on the Resulting Microstructure and Mechanical Properties of the Case Hardening Steel 16MnCr5 processed by Laser Powder Bed Fusion. *Procedia CIRP* **2021**, *104*, 726–731. [[CrossRef](#)]
3. Bartels, D.; Fallqvist, M.; Heise, M.; Vetter, J.; Schmidt, M.; Krakhmalev, P. Development of a novel wear-resistant WC-reinforced coating based on the case-hardening steel Bainidur AM for the substitution of carburizing heat treatments. *J. Mater. Res. Technol.* **2023**, *26*, 186–198. [[CrossRef](#)]
4. Liu, Y.; Zhang, J.; You, Q.; Zhang, L. A novel martensitic steel powder for plasma arc direct energy deposition to remanufacture broken gear teeth. *Mater. Lett.* **2021**, *301*, 130111. [[CrossRef](#)]
5. Edun, B.M.; Ajayi, O.O.; Babalola, P.O.; Salawu, E.Y. Effect of case hardening on the wear and hardness properties of medium carbon steel for bone crushing application. *Heliyon* **2023**, *9*, e17923. [[CrossRef](#)] [[PubMed](#)]
6. Kayiwa, R.; Kasedde, M.L.H.; Kirabira, J. The potential for commercial scale production and application of activated carbon from cassava peels in Africa: A review. *Bioresour. Technol. Rep.* **2021**, *15*, 100772. [[CrossRef](#)]
7. Oliver, G.D.; Cooke, K. An example of the infusion of endogenous technology in engineering curricula: The case hardening of mild steel using local Jamaica blue mountain coffee shells. In *World Transactions on Engineering and Technology Education; Engineering and Technology Education*: Kingston, Jamaica, 2005.
8. Ihom, P.A. Case hardening of mild steel using cowbone as energiser. *Afr. J. Eng. Res.* **2013**, *1*, 97–101.
9. Akanji, O.L.; Fatoba, O.S.; Aasa, A.S. The Influence of Particle Size and Soaking Time on Surface Hardness of Carburized AISI 1018 Steel. *Br. J. Appl. Sci. Technol.* **2015**, *7*, 37–44. [[CrossRef](#)]
10. Ibronke, O.J.; Falaiye, A.; Ojumu, T.V.; Odo, E.A.; Adewoye, O.O. Case-Depth Studies of Pack Cyaniding of Mild Steel Using Cassava Leaves. *Mater. Manuf. Process.* **2004**, *19*, 899–905. [[CrossRef](#)]

11. Sun, Y. Kinetics of low temperature plasma carburizing of austenitic stainless steels. *J. Mater. Process. Technol.* **2005**, *168*, 189–194. [[CrossRef](#)]
12. Wang, C.; Mandelis, A. Case depth determination in heat-treated industrial steel products using photothermal radiometric interferometric phase minima. *NDTE Int.* **2007**, *40*, 158–167. [[CrossRef](#)]
13. Katsamas, A.; Haidemenopoulos, G. Surface hardening of low-alloy 15CrNi6 steel by CO₂ laser beam. *Surf. Coat. Technol.* **1999**, *115*, 249–255. [[CrossRef](#)]
14. Sathishkumar, K.; Sowmiya, K.; Pragasan, L.A.; Rajagopal, R.; Sathya, R.; Ragupathy, S.; Krishnakumar, M.; Reddy, V.R.M. Enhanced photocatalytic degradation of organic pollutants by Ag–TiO₂ loaded cassava stem activated carbon under sunlight irradiation. *Chemosphere* **2022**, *302*, 134844. [[CrossRef](#)] [[PubMed](#)]
15. Cock, J. *Cassava: New Potential for a Neglected Crop*; Westview Press: Boulder, CO, USA, 1985.
16. Arthur, E.K.; Azeko, S.T. Surface hardening of ferrous materials with cassava (*Manihot* spp.) waste: A review. *Sci. Afr.* **2020**, *9*, e00483. [[CrossRef](#)]
17. Watchamongkol, T.; Khaopueak, P.; Seesau, C.; Wechakorn, K. Green Hydrothermal Synthesis of Multifunctional Carbon Dots from Cassava Pulps for Metal Sensing, Antioxidant, and Mercury Detoxification in Plants. *Carbon Resour. Convers.* **2023**, *2023*, 100206. [[CrossRef](#)]
18. Qiu, Y.; Wang, F.; Ma, X.; Yin, F.; Li, D.; Li, J. Carbon quantum dots derived from cassava stems via acid/alkali-assisted hydrothermal carbonization: Formation, mechanism and application in drug release. *Ind. Crops Prod.* **2023**, *204*, 117243. [[CrossRef](#)]
19. Amakoromo, T.; Abumere, O.; Amusan, J.; Anye, V.; Bello, A. Porous carbon from *Manihot Esculenta* (cassava) peels waste for charge storage applications. *Curr. Res. Green Sustain. Chem.* **2021**, *4*, 100098. [[CrossRef](#)]
20. Kayiwa, H.K.R.; Lubwama, M.; Kirabira, J. Characterization and pre-leaching effect on the peels of predominant cassava varieties in Uganda for production of activated carbon. *Curr. Res. Green Sustain. Chem.* **2021**, *4*, 100083. [[CrossRef](#)]
21. Jørgensen, K.; Morant, A.V.; Morant, M.; Jensen, N.B.; Olsen, C.E.; Kannangara, R.; Motawia, M.S.; Møller, B.L.; Bak, S. Biosynthesis of the Cyanogenic Glucosides Linamarin and Lotaustralin in Cassava: Isolation, Biochemical Characterization, and Expression Pattern of CYP71E7, the Oxime-Metabolizing Cytochrome P450 Enzyme. *Plant Physiol.* **2011**, *155*, 282–292. [[CrossRef](#)]
22. Zagrobelnya, M.; Bak, S.; Rasmussen, A.V.; Jørgensen, B.; Naumann, C.M.; Møller, B.L. Cyanogenic glucosides and plant–insect interactions. *Phytochemistry* **2004**, *65*, 293–306. [[CrossRef](#)]
23. Narayanan, N.; Ihemere, U.; Ellery, C.; Sayre, R.T. Overexpression of Hydroxynitrile Lyase in Cassava Roots Elevates Protein and Free Amino Acids while Reducing Residual Cyanogen Levels. *PLoS ONE* **2011**, *6*, e21996. [[CrossRef](#)] [[PubMed](#)]
24. Siritunga, D.; Arias-Garzon, D.; White, W.; Sayre, R.T. Over-expression of hydroxynitrile lyase in transgenic cassava roots accelerates cyanogenesis and food detoxification. *Plant Biotechnol. J.* **2004**, *2*, 37–43. [[CrossRef](#)] [[PubMed](#)]
25. Lee, S.-J.; Matlock, D.K.; Van Tyne, C.J. Carbon diffusivity in multi-component austenite. *Scr. Mater.* **2011**, *64*, 805–808. [[CrossRef](#)]
26. Pous-Romero, H.; Bhadeshia, H.K.D.H. Coalesced Martensite in Pressure Vessel Steels. *ASME J. Press. Vessel Technol.* **2014**, *136*, 031402-1-6. [[CrossRef](#)]
27. Arvanitidis, S.S. A Study of the Thermal Decomposition of BaCO₃. *Metall. Mater. Trans. B* **1996**, *27B*, 409–416. [[CrossRef](#)]
28. Sugianto, A.; Narazaki, M.; Kogawara, M.; Shirayori, A.; Kim, S.-Y.; Kubota, S. Numerical simulation and experimental verification of carburizing-quenching process of SCr420H steel helical gear. *J. Mater. Process. Technol.* **2009**, *209*, 3597–3609. [[CrossRef](#)]
29. Sarikaya, Y.; Onal, M. High temperature carburizing of a stainless steel with uranium carbide. *J. Alloys Compd. J.* **2012**, *542*, 253–256. [[CrossRef](#)]
30. Grube, W.L.; Gay, J.G. High-rate carburizing in a glow- discharge methane plasma. *Metall. Trans. A* **1978**, *9*, 1421–1429. [[CrossRef](#)]

Disclaimer/Publisher’s Note: The statements, opinions and data contained in all publications are solely those of the individual author(s) and contributor(s) and not of MDPI and/or the editor(s). MDPI and/or the editor(s) disclaim responsibility for any injury to people or property resulting from any ideas, methods, instructions or products referred to in the content.